Available online at www.sciencedirect.com
SCIENCE DIRECT®
Journal of Power Sources 149 (2005) 33–43
JOURNAL OF POWER SOURCES
www.elsevier.com/locate/jpowsour

Experimental analysis of the CHP performance of a PEMFC stack by a 2^4 factorial design

M.F. Torchio, M.G. Santarelli*, A. Nicali

Dipartimento di Energetica, Politecnico di Torino, Corso Duca degli Abruzzi 24, Torino 10129, Italy

Received 4 August 2004; received in revised form 24 January 2005; accepted 31 January 2005
Available online 22 March 2005

Abstract

The aim of the paper is the experimental analysis, through a statistical methodology, of the effects of the main stack operation independent variables on the cogenerative performance of a PEMFC stack. The tests have been performed on a ZSW 0184 stack of 800 W using the GreenLight GEN VI FC Test Station. The statistical methodology used for the experimental data analysis has been the factorial design: we have analysed the significance of the main operation independent variables (anode and; cathode flow dew point temperature; cathode flow stoichiometry) considering their single and combined effects on the electric and thermal power which could be recovered from the stack. The results show that the anode flow inlet temperature and the cathode flow dew point temperature have no significant effect at every level of current density both for electric and thermal power. At the same time, the cathode flow inlet temperature has a significant positive effect on the electric power at every level of current density, and especially the cathode flow stoichiometry shows significant positive effects on the electric power and negative effects on the thermal power recovered from the stack.
© 2005 Elsevier B.V. All rights reserved.

Keywords: PEMFC stack; Experimental analysis; Factorial design; CHP

1. Introduction

Up to now, most publications about PEMFC research mainly focused on a single cell or emphasized a single part of a fuel cell. These papers discuss fundamental scientific topics of the principal cell elements: proton conducting membrane (with particular attention to ionic conductivity and water transport mechanisms), catalyst layer, diffusion layer, electrochemical reactions. The papers describe the results of experimental analysis, or the development of modelling studies. Some other papers are devoted to the activity concerning PEMFC stacks. In this case too, the research activity describes experimental analysis, modelling studies and models development validated with experimental measurements.

1.1. Modelling studies

In literature, the papers dealing with the modelization of a whole stack are not predominant, compared to the modelization of a single cell and to the experimental characterization of a stack. In many cases parametric models are developed, with empirical modelling techniques and mechanistic equations. In some cases, the developed model is validated through experimental activity, allowing the determination of some model parameters: in [1], after the description of a detailed steady-state parametric electrochemical model of the Ballard Mark IV stack, the correlation of the empirical model to actual experimental data (28 runs experiment covering a range of operating currents, temperatures, oxygen partial pressures and hydrogen partial pressures) was used to find the model parameters. After, in [2] the authors extended the electrochemical model to include a thermal model of the Ballard Mark V 5 kW stack, and they pass from a steady-state to a transient model with output stack voltage, power and temperature both in

* Corresponding author. Tel.: +39 011 564 4487; fax: +39 011 564 4499.
E-mail addresses: marco.torchio@polito.it (M.F. Torchio), massimo.santarelli@polito.it (M.G. Santarelli), alnical@tin.it (A. Nicali).

0378-7753/$ – see front matter © 2005 Elsevier B.V. All rights reserved.
doi:10.1016/j.jpowsour.2005.01.060

Nomenclature

A	symbol of the factor $T_{H_2,in}$
B	symbol of the factor $T_{Air,in}$
C	symbol of the factor $T_{Air,DP}$
CHP	heat and power cogeneration
D	symbol of the factor λ_{Air}
DPT	differential pressure sensor
FCV	control valve
FM	flow meter
i	current density (A cm^{-2})
k	number of factors in the factorial analysis
MFC	mass flow controller
PEMFC	proton exchange membrane fuel cell
PT	pressure sensor
RH	relative humidity of the reactant flows (%)
$T_{Air,DP}$	cathode dew point inlet temperature (°C)
$T_{Air,in}$	cathode inlet temperature (°C)
$T_{H_2,in}$	anode inlet temperature (°C)
TC	thermocouple
w	effect of a factor evaluated through the Yates' technique

Greek letter

λ_{Air}	cathode stoichiometry

steady-state operation and as a function of time. In [3], a technique for numerically modelling the electrochemical performance of a MEA, developed specifically to be implemented as part of a general numerical model of a complete stack, is presented; after, in [4], the authors described the utilisation of the stack model to investigate the system parameters, along with the results of an investigation designed to test the validity of the technique on a four cells 50 cm^2 stack. In [5], empirical equations describing the polarization curves behaviour of a stack are presented, and used to model the experimental results at various humidity and temperatures of a air-breathing stack; in [6], the authors presented other empirical equations describing the transient voltage–time behaviour of a stack at constant current discharge, used to model the experimental results at different discharge currents and ambient temperature. In [7], a non-linear mathematical model (in Simulink) for investigating the dynamic performance of a PEMFC stack has been described, and the transient behaviour of the voltage within each single cell and in the whole stack has been displayed. In [8], an exergy analysis of a 10 kW stack at variable operating temperatures, pressures, cell voltages and air stoichiometries is described.

Some papers discuss the model of a whole plant with a stack connected with other components: in [9], a heat exchanger network (reformer, burner, gas cleaning, hot water storage and PEMFC stack) working under stationary conditions is modelled and designed using pinch technology, in order to evaluate the heat and power efficiencies of the system; in [10], a mathematical model of a FC/CHP system (unit converting natural gas to electricity and heat) has been developed to predict system performances and operating parameters under off-design conditions, used to optimize system operation to a particular customer, and validated through experiments aimed at assessing the suitability of the system.

Finally, some papers deals with the modelization of stacks embedded in a complete automotive system: in [11], a model simulating the operation of all the component of a system for transportation (FC stack, air compressor, hydrogen supply, cooling system) is described, and two duty cycles are used to examine the performance of the baseline system and to evaluate the benefits of improving individual system components; in [12], a transient model of a stack embedded in a vehicle simulation software (Matlab-Simulink, zero-dimensional approach), allowing the investigation of operation in driving cycles, is described, with a simplified thermal model and the examination of the effects of maximum stack power, catalyst activity, water concentration in the channels.

1.2. Experimental activity

The experimental activity is the object of the majority of the literature papers. In many cases, the activity concerns the analysis of the performance of stack modifications (structure, materials, humidification strategies, etc.). The performance is expressed usually in the form of the polarization curve, thus making the stack operate at variable load (not representative of a specific application: residential, automotive, etc.). In [13], a 5 kW PEMFC stack consisting of three 1.7 kW modules has been demonstrated, and the results of R&D activities are described (development of a method for the electrode preparation, enhancement of platinum utilisation using low platinum loading, design of multicell stacks). In [14], three types of stack structure of PEMFC are evaluated in various conditions: bipolar plate (best suitable for a high power supply); pseudo-bipolar plates (best suitable for low to moderate power sources); monopolar plate (best suitable for low power and high voltage devices). In [15], a 1 kW class fuel cell module operating on an exclusive method of internal humidification (with concurrent flows of hydrogen and water through the fuel gas passage in the fuel cell module) is described, also in start-up conditions (transient behaviour). In [16], the behaviour and performance of a stack under fast load commutations are described in form of polarization curves, energy balances sheet, and time response of the fuel cells; moreover, two literature models are used to fit the results. In [17], the performance of a 3 kW stack at four power levels is described in form of thermodynamic analysis (first and second law) of the results. In [18], a parametric study of a double-cell stack using Grafoil (flexible graphite) flow-field plates is described (effect of cell temperature, pressure and humidity of the reaction side, and flow-field geometry) through voltage-current and power-current curves, and two empirical correlations are developed and used to fit the results. In [19], the performance of a counter-flow type stack

Fig. 1. ZSW PEMFC 0184 stack.

is investigated with electron probe micro-analyser (EPMA) and X-ray fluorescence (XRF) spectrometer analysis, which revealed that degradation of the catalyst and contamination of the polymer electrolyte membrane were the main causes of a sudden decay after continuous operation of 1800 h. In [20], a double-path-type flow-field design with two gas inlets and two gas outlets (enabling the dry entering gas to become hydrated by acquiring some moisture from the exiting moist gas) is presented, and its effectiveness is demonstrated by running a four-cell stack (27.6 cm^2 active area) stably at current density of 0.33 A cm^{-2} using dry hydrogen and dry air. Giddey et al. first [21] described a test facility established to study fuel quality issues, start, stop, thermal cycling and load following capabilities of stacks up to 3 kW, then [22] described the results obtained on a stack of 1 kW, observing an increase in the ohmic resistance and a degradation of the electrical output of the stack. In [23], there is a description of test on a stack concept using graphite composite bipolar plates, through the analysis of the polarization curves varying the operating curves, the anode gas composition and the gas utilisation. In [24], an uniformity analysis is performed on the load of 800 W in 10 individual Nexa stacks at MEA and stack level; this analysis reveals a MEA voltage difference especially pronounced around the two cells at the air compressor side.

Some papers are devoted especially in stack tests with automotive loads. In [25], experimental water and thermal balances with three stacks (1 kW with Nafion 117; 5 kW and 10 kW with Nafion 115) are performed, showing the possibility of operation at low pressure without external humidification (important for the automotive industry). In [26], the paper investigates some aspects critical to the operation of large stacks in automotive applications such as control issues in the supply system, stack failures (negative voltage, leaks in the membrane, large differential pressure) and the appropriate countermeasures (current pulsing, flow and pressure pulsing, differential pressure across the membrane). In [27], the paper presents a test platform for automotive fuel cell systems and report some tests results on the various components (FC stack, motor, dc/dc converter). Finally, in [28] there is a description of an experimental analysis of the effect of some operation independent variables (hydrogen and oxygen pressures and flow rates) on the electric power output of a stack, supported by a statistical methodology.

1.3. Aims of the paper

The aim of our paper is the experimental analysis, through a statistical methodology, of the single and combined effects of the main stack operation independent variables on the cogenerative (electricity and heat) performance of a PEMFC stack.

The tests have been performed on a ZSW 0184 stack of 800 W (see [23]) using the GreenLight GEN VI FC Test Station.

The statistical methodology used for the experimental data analysis has been the factorial design (Yates' technique): using analysis of variance (ANOVA) we have analysed the significance of the main operation independent variables (factors: anode and cathode flows inlet temperature; cathode flow dew point temperature; cathode flow stoichiometry) considering their single and combined effects on the electric and thermal power which could be recovered from the stack.

2. PEMFC stack analysed

The tests have been made on a PEMFC stack of 800 W developed by ZSW (Zentrum für Sonnenenergie-und Wasserstoff-Forschung) [29]. The main characteristics are:

- Electric power: ∼800 W_e.
- Number of cells in series: 30.
- Cell active area: 100 cm^2.
- Cooling water flow: 1.6 N l min^{-1}.
- Current peak value: 50 A (0.5 A cm^{-2}).

A image of the stack is shown in Fig. 1.

Before testing, all the hoses in and out of the cell have been thermally insulated with ceramic canvas foils.

The stack characteristic has been obtained running a predefined loading pattern and setting the system in automatic mode. Parameters have been set in accordance with the constructor's data sheets (e.g.: stack operation temperature 55 °C; cathode stoichiometry 4).

3. Fuel cell test station

The test station provided by GreenLight is an inspection platform for PEMFC stacks up to 10 kW_e [30,31].

The test station modules are:

- *Gas supply module*: it allows to control and manage the reactants flows and pressures from the stack distribution network; this module also controls the inert gases bleeding when the system is in Safe Mode.
- *Input/output control module*: it works as an interface between the control PC and the modules constituting the station; it sends data to the control devices in the respective modules and receives information from the modules instruments.
- *Power distribution subsystem*: it provides both low voltage control wiring and high voltage distribution for ac motors, heaters, transformers and power supplies.
- *Humidification module*: it humidifies the reactant gases and controls the dew point and relative humidity of the gases entering the fuel cells. Heating/cooling and control of the temperature of the gases going through the stack is also available.
- *Fuel cell interface*: it is constituted by pressure transducer and thermocouples which link the fuel cells stack to the cells voltage monitoring subsystem.
- *Stack coolant module*: it has the function to warm up the stack during the start-up and to control the temperature during the running phase; this module employs a coolant loop and a servo-valve which controls the temperature of the coolant at the stack inlet to keep it within the fixed threshold.
- *Stack analytical function*: comprises the electronic load bank and the cells voltage monitor; the former controls the electronic load imposed to the stack dynamically (manual mode) or through a preset profile (automatic mode), the latter is used to verify the correct activity of all the cells forming the stack.

In Fig. 2, the scheme of the stack interface module is shown.

Concerning the hydrogen ducts (dotted lines), two mass flow controllers, with different flow range (MFC-131 and MFC-132), are available. At the inlet of the stack, the temperature (thermocouple TC-412) and the pressure (PT-411) are measured. The stack outlet temperature is measured too (TC-413), and a differential pressure meter (DPT-411) measures the pressure difference between fuel inlet and outlet. A similar system is replicated for the air ducts (dashed lines).

The cooling system (solid lines) uses de-ionized water, and it is equipped by a tank reservoir, a pump, a heater and a liquid–liquid heat exchanger, used to control the stack inlet temperature of the cooling flow. The cell inlet temperature of the coolant is controlled by the thermocouple (TC-264), the water flow is regulated by a control valve (FCV-261) and measured by a flow meter (FM-261), and the outlet temperature is measured by the thermocouple (TC-262). The differential pressure is also measured by the sensor DPT-461.

4. Methodology and experimental design

The electrical and heat power output of a PEMFC stack are influenced by several independent variables (hereafter defined as *factors)*, and to analyse their reciprocal influence an experimental design methodology is fundamental. In this work a full factorial design of experiments has been employed: an output variable could be correlated to the input variables (factors) pointing out their effect. So it is possible to find which factors deserve a particular attention: for example, a further analysis could be done or, if they are measurable variables, more accuracy could be necessary. At the contrary, the factors having a negligible effect could even be not considered in subsequent analysis. Also, the combined effects among the factors can be assessed.

Once the k input factors have been chosen, it is fundamental to determine their range of variation (the experimental domain). If the experiments are performed only at the lower bound and the upper bound of the range of variation of the factors (that is, only two levels of the factor are considered) 2^k experiments are required. Each combination of different factor levels is called treatment; if the treatment is replicated, then an analysis of variance can be performed.

Concerning the adopted symbolism, each factor is labelled with a capital letter; to describe the treatments, a lowercase letter is used when the factor is at the upper level, while the letter is omitted when it is at its lower level; when all the factors are at the lower level, the notation (L) is used. To analyse the effects of the main factors the well-known Yates' technique has been employed: the treatment combinations must be therefore written down in standard form [32,33]. The effects of the factors (indicated with the letter w), are distinguished in main effects (w_A, w_B, ...), and interaction effects (w_{AB}, w_{AC}, ...).

In the experiment session discussed in the paper, four factors have been chosen, with two test replications. Therefore, a total of $2^4 \times 2 = 32$ experiment has been necessary to ob-

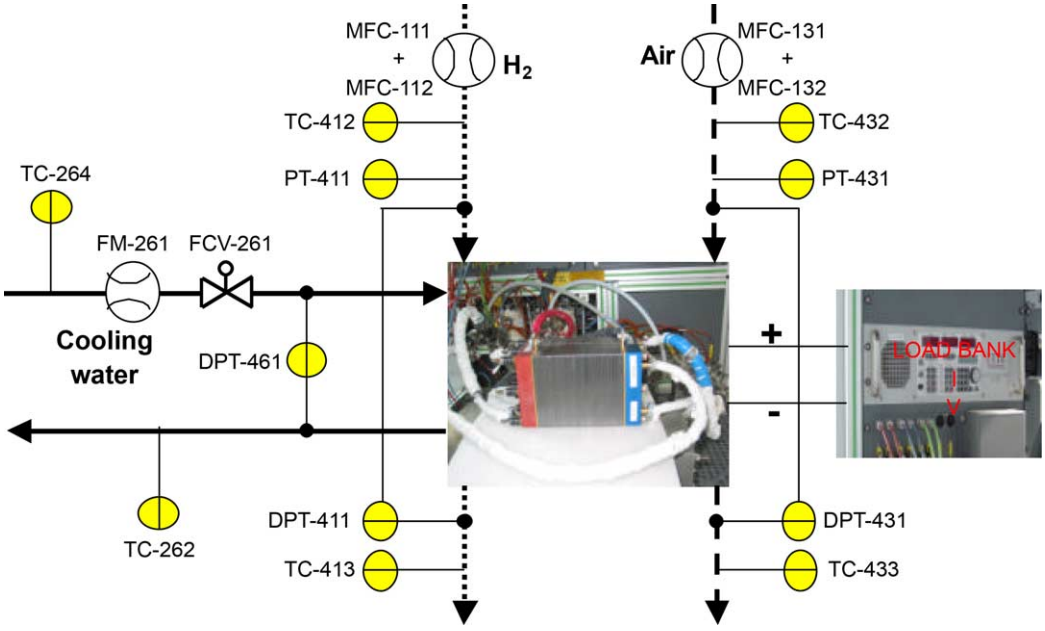

Fig. 2. Scheme of the stack interface module (TC: thermocouple; PT: pressure transducer; DPT: differential pressure transducer; MFC: mass flow controller; FM: flow meter; FCV: flow control valve).

Table 1
Factors analysed (each factor is labelled with a capital letter) and their levels

Factor	Description	Lower level (−)	Upper level (+)
A	$T_{H_2,in}$ (°C)	25	55
B	$T_{Air,in}$ (°C)	25	55
C	$T_{Air,DP}$ (%)	50	100
D	λ_{Air}	3	4

tain all the possible effects and interactions. The four factors chosen have been: anode inlet temperature $T_{H_2,in}$, cathode inlet temperature $T_{Air,in}$, cathode dew point inlet temperature $T_{Air,DP}$, cathode stoichiometry λ_{Air}.

The range of the factors is shown in Table 1.

Concerning the inlet temperature, the lower level is the ambient temperature, while the upper level is imposed by the stack temperature. To assure enough water inlet for the membrane hydration, the lower value for the cathode dew point is not fixed at dry conditions, but at a relative humidity of 50%, while the upper level is at a relative humidity of 100%. Concerning the upper level of the cathode stoichiometry, the recommend value for the analysed stack (4) has been adopted, and the lower level has been imposed to (3).

Two output are investigated in this work: the thermal and electrical power of the PEMFC stack. It is useful to study the performance of a stack through the polarization curve. To reduce the number of experiments, only three operating conditions has been analysed at three different current density values (0.2, 0.3, 0.4 A cm^{-2}). The load profile is shown in Fig. 3: a ramp of 0.167 A cm^{-2} was adopted and when the current reach 5 A the current was kept constant (short plateau) for 2 min. With four ramps and plateaux the chosen current density was reached and at this value a long plateau was kept: 10 min. The values of the measured variables adopted in the analysis was the mean in the last 5 min of this plateau (where the steady-state condition could be assumed as reached), and the sampling rate the data logging was fixed equal to 1 s. Then, another ramp and another plateau were imposed up to 0.3 and 0.4 A cm^{-2}. Finally, the test was concluded by a descending ramp. The total test length was ca. 50 min.

The factorial analysis was done at the indicated three current densities, both for electrical and heat power. During the tests, some parameters were kept constant: the inlet temperature of the cooling de-ionized water (55 °C), the humidity content of the hydrogen inlet flow (dry), and the hydrogen stoichiometry (2).

5. Results and discussion

To use the Yates' technique, the treatment combinations must be written down in standard form. These collected data are shown in Tables 2 and 3, where for each treatment and each current density two values of the dependent variables (one for each replication) are shown.

The thermal power is always smaller than the electric power (a fraction of the thermal power is lost to the environment and the reactant flows, and therefore the recovered thermal power is lower than the heat produced by stack irreversibility). It is possible to consider the average values (of all the treatments and replications, indicated at the bottom of the table) to present some indicative value: it could be said that from a stack operating at nearly 700 W_e (0.4 A cm^{-2})

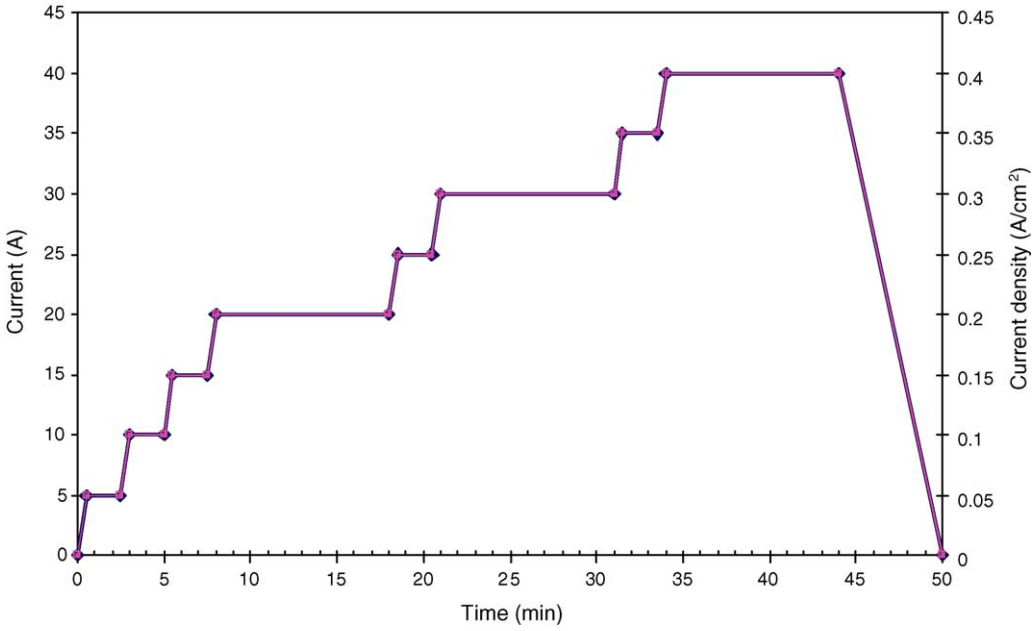

Fig. 3. Load profile imposed in the test session.

without thermal insulation it is possible to recover just around 330 W_{th} (47% of the electric power). Moreover, the relative gap increases at partial load: 39% at 0.3 A cm^{-2} and 19% at 0.2 A cm^{-2}. In fact, the average value of the thermal power obviously decreases at partial load (−40% at 0.3 A cm^{-2} and −80% at 0.2 A cm^{-2}); but it could be outlined that its relative reduction is higher than the corresponding relative reduction of the average electrical power (−27% at 0.3 A cm^{-2} and −52% at 0.2 A cm^{-2}).

More useful information could be obtained from a factorial design analysis.

An example of the calculation of effects and the analysis of variance for some results (electric power at current density of 0.2 A cm^{-2}) is shown in Table 4.

To discuss the results of the complete factorial design some diagrams concerning thermal and electric power have been drawn.

Starting from the thermal power, the full factorial design (Fig. 4) and its analysis of variance (Fig. 5) show that two single factors have significant effects at 99% confidence: the cathode inlet temperature (B) and the cathode stoichiometry (D). The other two factors (anode inlet tem-

Table 2
Thermal power obtained in each treatment (for each current density two replications are shown, and at the bottom of the table the average values are shown)

Treatment	$T_{H_2,in}$ (°C)	$T_{Air,in}$ (°C)	RH (%), $T_{Air,DP}$ (°C)	λ_{Air}	Thermal power (W)					
					0.2 A cm^{-2}		0.3 A cm^{-2}		0.4 A cm^{-2}	
(L)	25	25	50%, 14	3	40	33	224	202	349	306
a	55	25	50%, 14	3	82	55	208	218	319	325
b	25	55	50%, 14	3	90	86	252	212	399	318
ab	55	55	50%, 41	3	103	124	242	236	355	376
c	25	25	100%, 25	3	90	76	243	189	374	303
ac	55	25	100%, 25	3	98	75	210	230	316	332
bc	25	55	100%, 55	3	136	83	272	231	435	418
abc	55	55	100%, 55	3	107	108	259	269	406	390
d	25	25	50%, 14	4	25	7	144	122	261	257
ad	55	25	50%, 14	4	43	24	155	143	275	270
bd	25	55	50%, 41	4	65	35	178	153	315	289
abd	55	55	50%, 41	4	49	57	158	165	298	290
cd	25	25	100%, 25	4	37	3	139	107	267	229
acd	55	25	100%, 25	4	62	37	183	148	295	257
bcd	25	55	100%, 55	4	84	58	218	195	370	349
abcd	55	55	100%, 55	4	72	73	218	184	365	335
Average value					66		197		326	

Table 3
Electric power obtained in each treatment (for each current density two replications are shown, and at the bottom of the table the average values are shown)

Treatment	$T_{H_2,in}$ (°C)	$T_{Air,in}$ (°C)	RH (%), $T_{Air,DP}$ (°C)	λ_{Air}	Electric power (W)					
					0.2 A cm^{-2}		0.3 A cm^{-2}		0.4 A cm^{-2}	
(L)	25	25	50%, 14	3	360	344	449	445	654	646
a	55	25	50%, 14	3	277	322	447	431	665	648
b	25	55	50%, 14	3	316	291	476	472	669	671
ab	55	55	50%, 41	3	298	273	467	487	669	679
c	25	25	100%, 25	3	291	288	436	450	664	656
ac	55	25	100%, 25	3	280	319	459	439	667	659
bc	25	55	100%, 55	3	283	310	495	481	676	657
abc	55	55	100%, 55	3	370	320	573	483	752	655
d	25	25	50%, 14	4	373	370	538	547	738	740
ad	55	25	50%, 14	4	385	377	545	539	743	736
bd	25	55	50%, 41	4	382	367	562	571	745	749
abd	55	55	50%, 41	4	356	367	541	563	733	751
cd	25	25	100%, 25	4	351	366	551	569	744	747
acd	55	25	100%, 25	4	367	375	508	543	718	745
bcd	25	55	100%, 55	4	372	368	571	572	740	751
abcd	55	55	100%, 55	4	383	370	548	574	701	752
Average value					340		510		704	

perature (A) and cathode dew point inlet temperature (C)) have little significance, as well as all the combinations of factors.

When the cathode inlet temperature (B) increases, there is a positive effect on the recovered thermal power. At current densities of 0.2 and 0.3 A cm^{-2} the effects are close: 17 and 18 W, respectively. At 0.4 A cm^{-2} the effects are more consistent: 30 W of increase. The importance of the air inlet temperature is due to the fact that, as the inlet stream is already hot, it absorbs a lower heat amount from the stack interior walls; therefore, a higher heat amount is removed by the cooling water flow, thus increasing the thermal power recovered from the stack.

Analysing the cathode stoichiometry (D), when it increases the effect on thermal power is negative. In fact, a lower value means a reduced inlet air mass flow, and therefore a higher heat amount is removed by the cooling water. This effect is more strong at current density of 0.3 and 0.4 A cm^{-2} (−34 W and −31 W, respectively), and it is slightly reduced at 0.2 A cm^{-2} (−20 W).

It is also useful to observe the effects evaluated as percentage of the average values of thermal power at every current density (66 W at 0.2 A cm^{-2}, 197 W at 0.3 A cm^{-2} and 326 W at 0.4 A cm^{-2}). The percentage increase of the thermal power due to B is maximum at 0.2 A cm^{-2} (26%), while it is similar at 0.3 and 0.4 A cm^{-2} (9%). At the same time, the negative influence of D on the recovered thermal power is reduced at high current densities: in fact, the percentage decreases of thermal power are −31%, −17% and −10% at 0.2, 0.3 and 0.4 A cm^{-2}, respectively.

Table 4
Yates' technique applied for the analysis of the effects on the electric power with current density of 0.2 A cm^{-2}, analysis of variance

Treatment	Total treatment	(1)	(2)	(3)	(4)	Effect	dof	Mean square	Computed f
(L)	704	1302.6	2480.6	4940.8	10867.6	679.22	1		
a	599	1178.0	2460.2	5926.8	5.5	0.34	1	0.95	0.00
b	607	1177.5	2976.3	−24.3	−17.5	−1.09	1	9.53	0.03
ab	571	1282.7	2950.5	29.8	87.9	5.49	1	241.52	0.85
c	579	1504.3	−140.2	−19.4	−46.2	−2.89	1	66.72	0.23
ac	599	1472.0	115.9	1.9	299.3	18.70	1	2798.51	9.79
bc	593	1458.1	−6.7	145.8	296.4	18.52	1	2745.27	9.61
abc	689	1492.4	36.5	−57.9	42.7	2.67	1	56.85	0.20
d	742	−104.8	−124.6	−20.4	986.1	61.63	1	30385.62	106.34
ad	762	−35.4	105.3	−25.8	54.1	3.38	1	91.57	0.32
bd	749	19.8	−32.3	256.1	21.3	1.33	1	14.14	0.05
abd	723	96.1	34.2	43.2	−203.6	−12.73	1	1295.75	4.53
cd	717	20.1	69.4	229.9	−5.5	−0.34	1	0.93	0.00
acd	741	−26.7	76.4	66.5	−212.9	−13.31	1	1416.81	4.96
bcd	740	23.8	46.8	6.9	−163.3	−10.21	1	833.82	2.92
abcd	753	12.7	−11.1	35.7	28.8	1.80	1	25.91	0.09

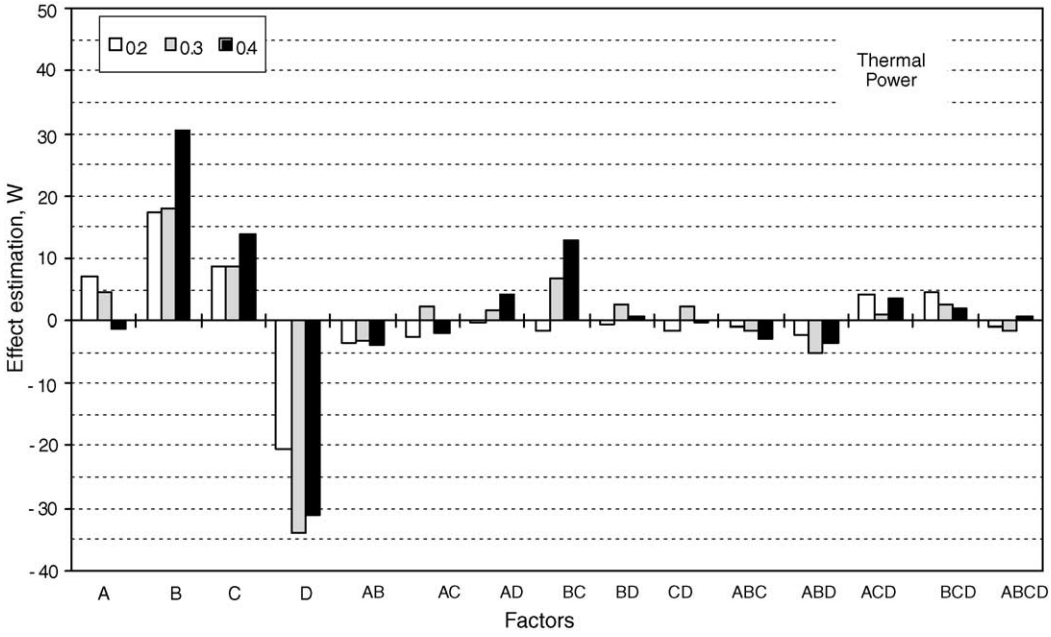

Fig. 4. Factorial analysis effect estimation on the thermal power.

Concerning the electric power, only the cathode stoichiometry shows always a significant effect (Figs. 6 and 7).

At the contrary compared to the thermal power behaviour, the increase of the cathode stoichiometry has a positive effect on the electric power. This behaviour could be due to a lower availability of the oxidant for the reaction in case of lower D value. Moreover, a bigger flow rate (high D) helps to remove the water generated from the reaction and so reduces the cathode side flooding risk. The effect of D is more strong at current density of 0.4 A cm^{-2} (+42 W), while at 0.2 A cm^{-2} the effect is +31 W, and at 0.3 A cm^{-2} is +36 W. The relative effect of D on electric power is lower compared to the effect on thermal power: +9% at 0.2 A cm^{-2}, +8% at 0.3 A cm^{-2}, +5% at 0.4 A cm^{-2}.

The cathode inlet temperature has a significant effect only at 0.3 A cm^{-2} (+17 W).

In order to organize the obtained results, it is possible to characterize two possible situations, shown in Fig. 8.

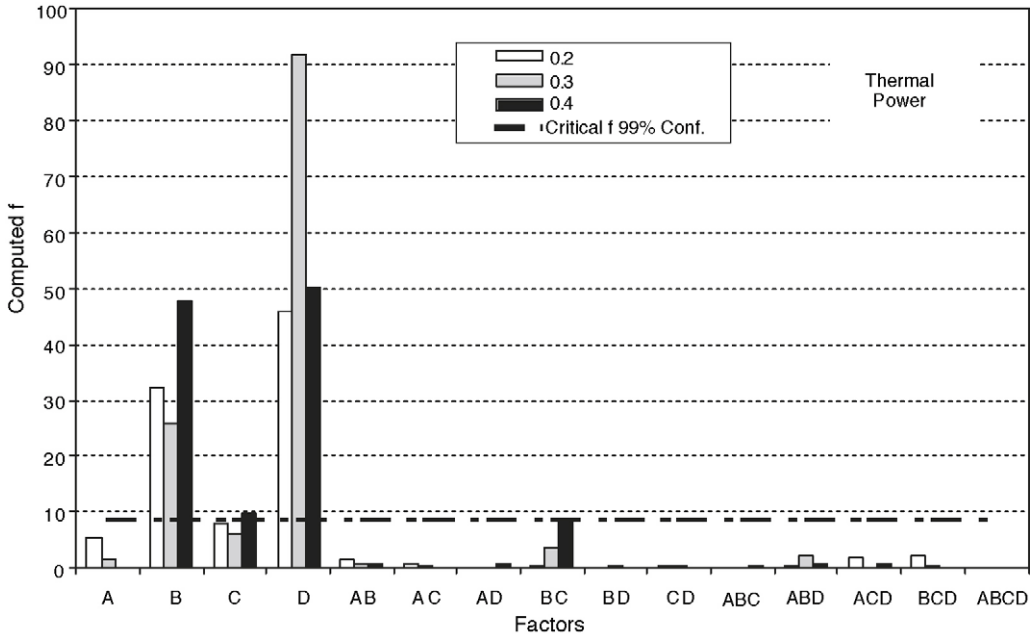

Fig. 5. Computed *f* of the significance of the factor effect on the thermal power.

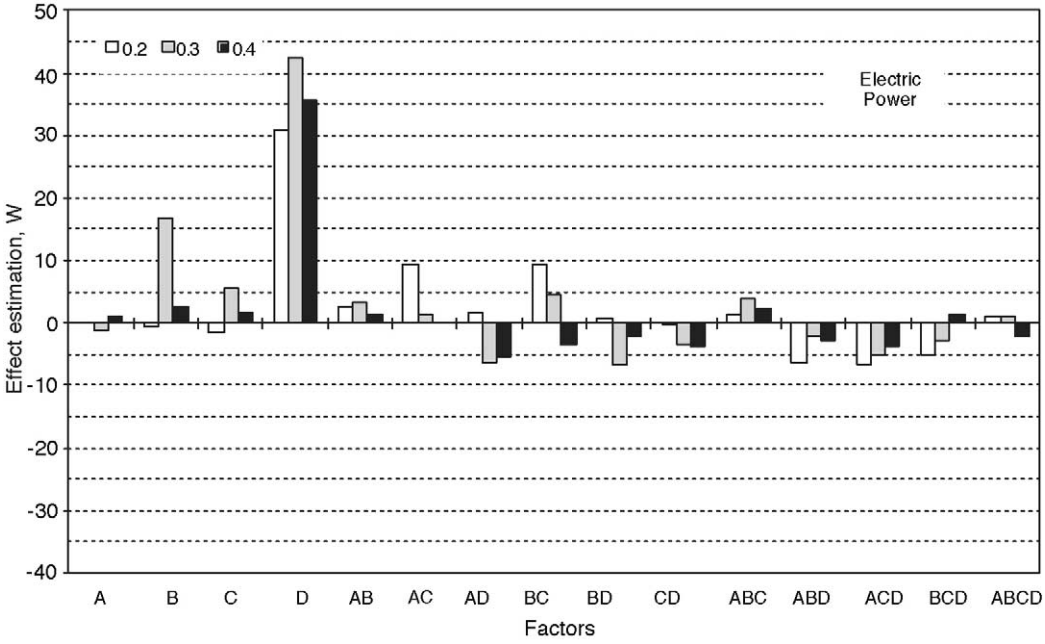

Fig. 6. Factorial analysis effect estimation on the electric power.

Fig. 8 shows the effect on the power behaviour (thermal dashed lines, and electrical solid lines) of the factors with high significance.

Concerning the factor B effect, its upper level (empty triangles) assures a significant improvement to both thermal and electrical power compared to its lower level (filled triangles). Moreover, as Fig. 8 shows, the variation of the cathode stoichiometry (D) can be used to obtain two results: reducing D, we obtain an improvement of the thermal power with an electrical power detriment (empty triangles); increasing D, we obtain an improvement of the electrical power with a thermal power detriment (empty circles). These behaviour is similar for all the current densities in the range analysed (0.2–0.4 A cm^{-2}), and it could be used in order to optimize the plant operation at different load situations.

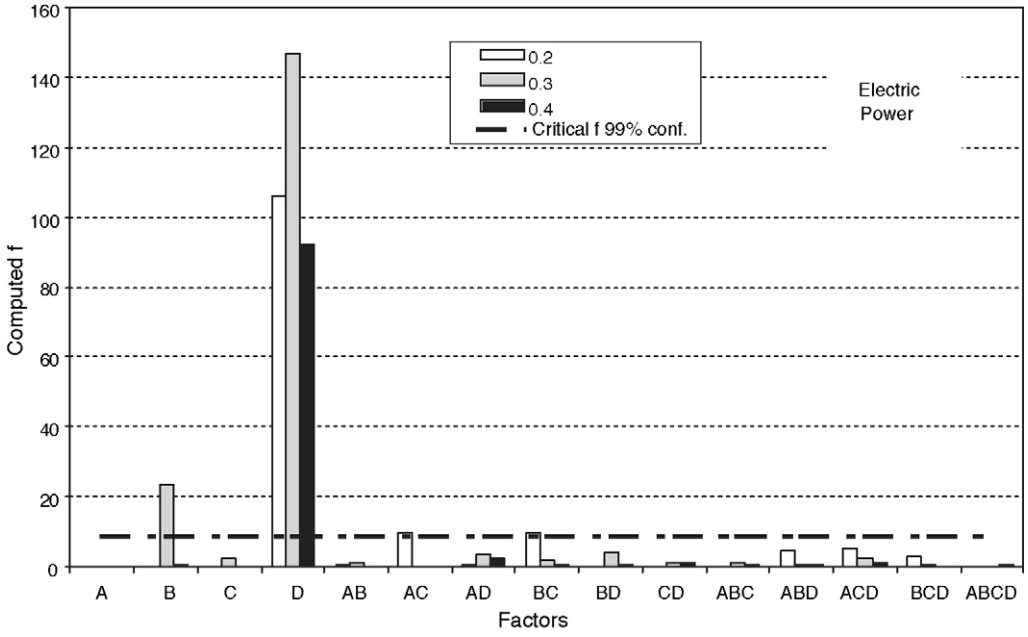

Fig. 7. Computed *f* of the significance of the factor effect on the electric power.

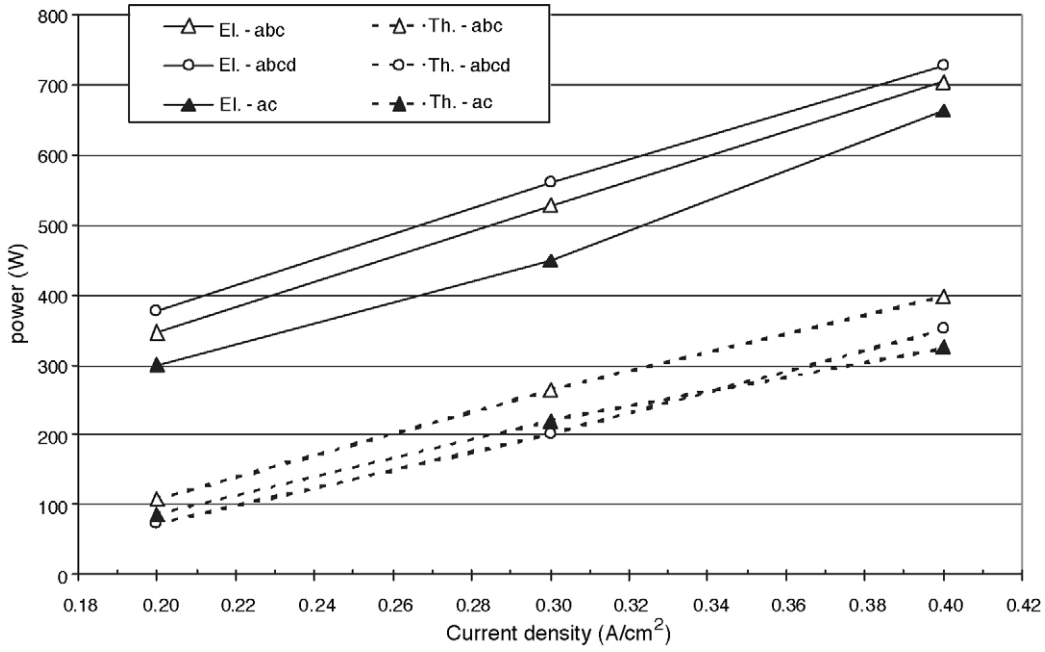

Fig. 8. Thermal power (dashed line) and electric power (solid line) vs. current density for the treatment "ac" (filled triangles), "abc" (empty triangles) and "abcd" (empty circles).

6. Conclusions

In this paper, the experimental analysis, through a statistical methodology, of the single and combined effects of the main stack operation independent variables (anode and cathode flows inlet temperature; cathode flow dew point temperature; cathode flow stoichiometry) on the cogenerative performance of a PEMFC stack has been performed. The results can be summarized as follows:

- the factorial design is a powerful tool to analyse the significance of the modifications of the main operation independent variables of a stack;
- the anode flow inlet temperature and the cathode flow dew point temperature have no significant effect at every analysed level of current density both for electric and thermal power;
- the increase of the cathode flow inlet temperature has a significant positive effect (increment) on the electric power at every level of current density;
- the increase of the cathode flow stoichiometry causes a significant positive effects (increment) on the electric power, and its effect is more strong at high current density;
- the increase of the cathode flow stoichiometry causes a significant negative effects (decrement) on the thermal power recovered from the stack, especially at high current density;
- the modification of the cathode flow stoichiometry could be used in order to optimize the plant operation at different load situations;
- furthermore, it has been noticed the high amount of heat released by convection from the stack to the external environment: in subsequent tests, it would be necessary to add a thermal insulation of the stack.

Acknowledgments

The authors wish to thank the Hydrogen System Laboratory (HySyLab) of the Environment Park of Torino, and in particular E. Novo, for the experimental support of the present work.

References

[1] J.C. Amphlett, R.M. Baumert, R.F. Mann, B.A. Peppley, P.R. Roberge, Performance modeling of the Ballard Mark IV solid polymer electrolyte fuel cell, J. Electrochem. Soc. 142 (1995) 1–15.
[2] J.C. Amphlett, R.F. Mann, B.A. Peppley, P.R. Roberge, A. Rodrigues, A model predicting transient responses of proton exchange membrane fuel cells, J. Power Sources 61 (1996) 183–188.
[3] J.H. Lee, T.R. Lalk, A.J. Appleby, Modelling electrochemical performance in large scale proton exchange membrane fuel cell stacks, J. Power Sources 70 (1998) 258–268.
[4] J.H. Lee, T.R. Lalk, Modelling of fuel cell stack systems, J. Power Sources 73 (1998) 229–241.
[5] D. Chu, R. Jiang, Performance of polymer electrolyte membrane fuel cell (PEMFC) stacks. Part 1. Evaluation and simulation of an air-breathing PEMFC stack, J. Power Sources 83 (1999) 128–133.
[6] R. Jiang, D. Chu, Voltage–time behaviour of a polymer electrolyte membrane fuel cell stack at constant current discharge, J. Power Sources 92 (2001) 193–198.

[7] S. Yerramalla, A. Davari, A. Feliachi, T. Biswas, Modelling and simulation of the dynamic behaviour of a polymer electrolyte membrane fuel cell, J. Power Sources 124 (2003) 104–113.
[8] A. Kazim, Exergy analysis of a PEM fuel cell at variable operating conditions, Energy Convers. Manage. 45 (2004) 1949–1961.
[9] C. Wallmark, P. Alvfors, Design of stationary PEFC system configurations to meet heat and power demands, J. Power Sources 106 (2002) 83–92.
[10] G. Gigliucci, L. Petruzzi, E. Cerelli, A. Garzasi, A. LaMendola, Demonstration of a residential CHP system based on PEM fuel cells, J. Power Sources 131 (2004) 62–68.
[11] R. Cownden, M. Nahon, M.A. Rosen, Modelling and analysis of a solid polymer fuel cell system for transportation applications, J. Hydrogen Energy 26 (2001) 615–623.
[12] C.N. Maxoulis, D.N. Tsinoglou, G.C. Koltsakis, Modelling of automotive fuel cell operation in driving cycles, Energy Convers. Manage. 45 (2004) 559–573.
[13] K.S. Dhathathreyan, P. Sridhar, G. Sasikumar, K.K. Ghosh, G. Velayutham, N. Rajalakshmi, C.K. Subramaniam, M. Raja, K. Ramya, Development of polymer electrolyte membrane fuel cell stack, J. Hydrogen Energy 24 (1999) 1107–1115.
[14] R. Jiang, D. Chu, Stack design and performance of polymer electrolyte membrane fuel cells, J. Power Sources 93 (2001) 25–31.
[15] T. Susai, A. Kawakami, A. Hamada, Y. Miyake, Y. Azegami, Development of a 1 kW polymer electrolyte fuel cell power source, J. Power Sources 92 (2001) 131–138.
[16] J. Hamelin, K. Agbossou, A. Laperrière, F. Laurencelle, T.K. Bose, Dynamic behaviour of a PEM fuel cell stack for stationary applications, J. Hydrogen Energy 26 (2001) 625–629.
[17] R. Johnson, C. Morgan, D. Witmer, T. Johnson, Performance of a proton exchange membrane fuel cell stack, Int. J. Hydrogen Energy 26 (2001) 879–887.
[18] J.J. Hwang, H.S. Hwang, Parametric study of a double-cell stack of PEMFC using Grafoil^{TM} flow-field plates, J. Power Sources 104 (2002) 24–32.
[19] S.Y. Ahn, S.J. Shin, H.Y. Ha, S.A. Hong, Y.C. Lee, T.W. Lim, I.H. Oh, Performance and lifetime analysis of the kW-class PEMFC stack, J. Power Sources 106 (2002) 295–303.
[20] Z. Qi, A. Kaufman, PEM fuel cell stacks operated under dry-reactant conditions, J. Power Sources 109 (2002) 469–476.
[21] S. Giddey, F.T. Ciacchi, S.P.S. Badwal, V. Zelizko, J.H. Edwards, G.J. Duffy, A versatile polymer electrolyte membrane fuel cell (3 kW_e) facility, Solid State Ionics 152/153 (2002) 363–371.
[22] S. Giddey, F.T. Ciacchi, S.P.S. Badwal, Design, assembly and operation of polymer electrolyte fuel cell stacks to 1 kW_e capacity, J. Power Sources 125 (2004) 155–165.
[23] J. Scholta, N. Berg, P. Wilde, L. Jorissen, J. Garche, Development and performance of a 10 kW PEMFC stack, J. Power Sources 127 (2004) 206–212.
[24] W.H. Zhu, R.U. Payne, D.R. Cahel, B.J. Tatarchuk, Uniformity analysis at MEA and stack levels for aNexa PEM fuel cell system, J. Power Sources 128 (2004) 231–238.
[25] D. Picot, R. Metkemeijer, J.J. Bezian, L. Rouveyere, Impact of the water symmetry factor on humidification and cooling strategies for PEM fuel cell stacks, J. Power Sources 75 (1998) 251–260.
[26] P. Rodatz, F. Buchi, C. Onder, L. Guzzella, Operational aspect of a large PEFC stack under practical conditions, J. Power Sources 128 (2004) 208–217.
[27] P. Pei, M. Ouyang, Q. Lu, H. Huang, X. Li, Testing of an automotive fuel cell system, J. Hydrogen Energy 29 (2004) 1001–1007.
[28] R.C. Dante, J.L. Escamilla, V. Madrigal, T. Theuss, J.D. Calderon, O. Solorza, R. Rivera, Fractional factorial design of experiments for PEM fuel cell performance improvement, J. Hydrogen Energy 28 (2003) 343–348.
[29] Operation Manual PEM-FC-Stack, Zentrum fur Sonnenenergie-und Wasserstoff-Forschung, Baden-Wurttemberg, 2003.
[30] Fuel Cell Test Station Operating and Maintenance Guide, GreenLight Power Technologies, Vancouver, 2002.
[31] Fuel Cell Test Station Original Equipment Manufacturer Specification and Data Sheets, GreenLight Power Technologies, Vancouver, 2002.
[32] R.E. Walpole, R.H. Myers, Probability and Statistics for Engineers and Scientists, Prentice-Hall International Inc., New Jersey, 1993.
[33] J.V. Beck, K.J. Arnold, Parameter Estimation in Engineering and Science, John Wiley & Sons, New York, 1977.